Available online at www.sciencedirect.com
SCIENCE DIRECT®
ELSEVIER
Journal of Magnetism and Magnetic Materials 286 (2005) 51–55
Journal of magnetism and magnetic materials
www.elsevier.com/locate/jmmm

Domain wall propagation in continuous thin films initiated by precessional reversal

M. Kerekes[a], A.D.C. Viegas[a,b], D. Stanescu[a,c], U. Ebels[a,*], P. Xavier[c], L.S. Dornelles[b], R.L. Sommer[b]

[a]*URA 2512 SPINTEC, CEA/CNRS, CEA - Grenoble, 17 Av. Martyrs, 38054 Grenoble, France*
[b]*Departamento de Física, Universidade Federal de Santa Maria (UFSM), Brazil*
[c]*UMR 5130 IMEP CNRS-UJF-INPG, Grenoble, France , 23 Av des Martyrs, 38016 Grenoble, France*

Available online 12 October 2004

Abstract

Using time resolved magneto-optic Kerr effect magnetometry, the precessional reversal properties of continuous soft magnetic layers such as Permalloy and Finemet have been studied in the presence of a weak bias field applied parallel to the initial magnetisation direction. This configuration induces for appropriate pulse width and pulse height, a reversed domain with two domain walls. It will be shown how these time resolved studies can be used to investigate the wall velocity and wall mobility of in-plane magnetised thin films.

PACS: 75.60.Jk; 75.60.Ch; 78.47.De

Keywords: Ultrafast magnetisation reversal; Precessional reversal; Domain wall velocity; Relaxation

Recently, an ultrafast reversal mechanism has been predicted [1] and verified in a number of experiments [2–5]. This reversal is based on the precessional in-plane motion of the magnetisation in thin film elements, induced by an ultrafast field pulse oriented perpendicular to the magnetisation. Here, we present studies on the precessional reversal in the presence of a static bias field in soft continuous layers. It will be shown how the precessional reversal mechanism can be exploited in continuous thin films in order to study relaxation effects related to domain wall propagation.

Two types of continuous thin films have been prepared by sputtering on top of microscope cover slides. The first is a $Fe_{20}Ni_{80}$ (Py) film of 30 nm thickness, with a growth induced uniaxial anisotropy H_u of 8 Oe and an easy axis coercivity H_c of

*Corresponding author. Tel.: +33 438 78 5344; fax: +33 438 78 2127.
E-mail address: ebels@drfmc.ceng.cea.fr (U. Ebels).

0304-8853/$ - see front matter © 2004 Elsevier B.V. All rights reserved.
doi:10.1016/j.jmmm.2004.09.035

1.5 Oe. The second film is a precursor alloy for Finemet $Fe_{73.5}Cu_1Nb_3Si_{14.5}B_9$ of 50 nm thickness, with $H_u = 10$ Oe and $H_c = 1.7$ Oe.

For the time resolved magneto-optic Kerr effect studies, the films are placed face down on top of a high bandwidth coplanar waveguide (CPW), see Fig. 1, whose centreline is tapered to 10 μm in the middle of its length. This allows the application of sharp magnetic field pulses of 60 ps risetime and of up to 90 Oe amplitude. The dynamic response of the magnetisation is probed stroboscopically using a 20 ps duration laser pulse delivered by a diode laser. The laser beam is focused to a spot of 15 μm. The reflected light is detected synchronously using an optical bridge.

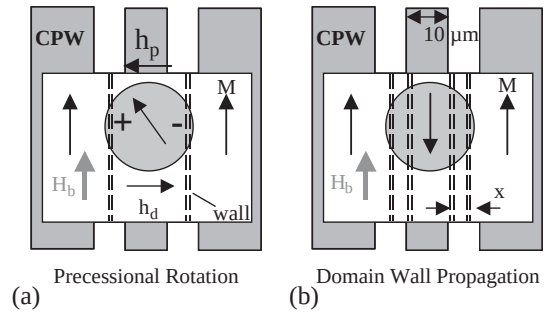

Fig. 1. Schematic of the measurement configuration of a continuous film on top of a CWG (a) appearance of dynamic magnetic charges, (b) wall propagation after one complete reversal.

With the anisotropy easy axis oriented perpendicular to the field pulse h_p, and with a strong enough h_p, the corresponding torque will induce an in-plane precessional reversal [1–5]. After pulse termination, the magnetisation will relax to its closest easy axis position, either parallel or antiparallel to the initial direction. For a given pulse width, the corresponding time evolution (time traces) of the magnetisation component parallel to the easy axis direction (Ku) is obtained by monitoring the Kerr signal for different time delays. Typical time traces for different pulse widths are shown in Fig. 2a for the Finemet sample and in Fig. 2b for the Py sample. These time traces indicate the first (left), the second (middle) and third (right) reversal regime, where the magnetisation switches from the initial $-M_s$ to the reversed $+M_s$ direction in $\frac{1}{2}$, $1\frac{1}{2}$ and $2\frac{1}{2}$ precession cycles, respectively. It is noted, that for the 2nd and 3rd reversal regime, the magnetisation performs multiple large angle oscillations, during which the magnetisation component parallel to K_u remains always smaller than $+M_s$. This means that the magnetisation does not perform a 360°

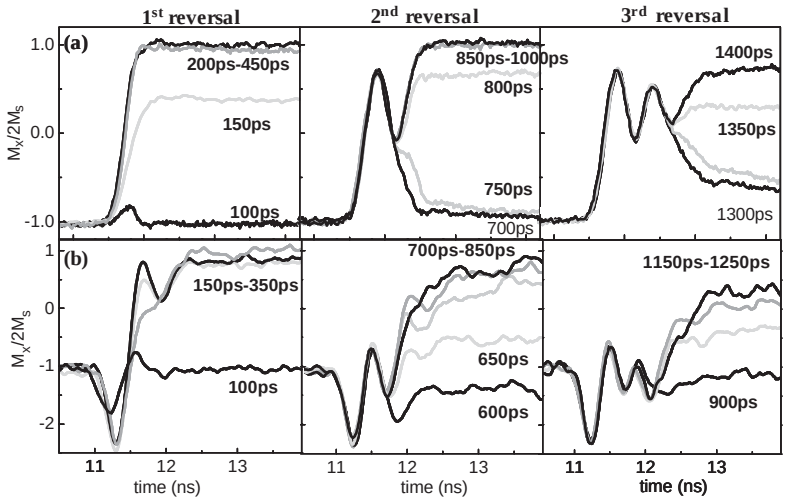

Fig. 2. Time traces of (a) the Finemet and (b) the Py thin film for Left: 1st reversal, Middle: 2nd reversal and Right: 3rd reversal regime. The pulsed field amplitude is 90 Oe. The undershoot seen in (b) beyond the static magnetisation level of −1 is attributed to an optical effect.

in-plane precession around the demagnetisation field (with constant sign of the out of plane component), but rather oscillates around the pumping field direction h_p upon changing sign of the out of plane component.

In the following, we will focus on the Py results. Comparison of the experimental minimum field pulse $h_{pmin} \approx 30$ Oe, required for reversal, with the theoretical value [6] $h_{pmin} = H_u/2 \approx 4$ Oe, shows that the experimental value is much larger for the pulse durations of 100 ps–1.5 ns investigated. To explain this apparent discrepancy, we have to consider that the precessional reversal is induced only along a stripe of ~10 μm width, see Fig. 1, while the magnetisation outside this excitation volume remains aligned along the initial magnetisation direction. Hence, the rotation is accompanied by dynamic charges at the boundary between the excited and non-excited volume, giving rise to an effective dynamic demagnetisation field $h_d(t) = N_y * M_y(t)$, that is equivalent to a uniaxial shape anisotropy of a long stripe. Comparison of the data with macrospin simulations give a good agreement for $N_y \approx 0.004$. This corresponds to an effective stripe width of about 18 μm, which is reasonable, since the reversal might partially extend into the gap region of the CWG. In the following we assume that the full area below the laser spot of 15 μm diameter is reversed.

Interesting effects can be observed, when applying an additional static bias field H_b, along the initial magnetisation direction. Depending on the field strength, the pulse width range where reversal occurs will be reduced or even suppressed.

More important are the relaxation effects which are apparent in Fig. 3b, c where time traces for different pulse durations are shown in the presence of a bias field of 1.6 Oe for the Py continuous film. It is noted that the stroboscopic measurement technique requires the resetting of the magnetisation to its initial direction after each initial field pulse. In our case this is achieved by the use of a second field pulse of same polarity and applied 10 ns after the first pulse. In consequence, in Fig. 3b, c, e, the transition from the initial to the reversed state is initiated at $t = 28$ ns, while the back-reversal is initiated at $t = 38$ ns. As can be seen in Fig. 3a, b, the magnetisation level between

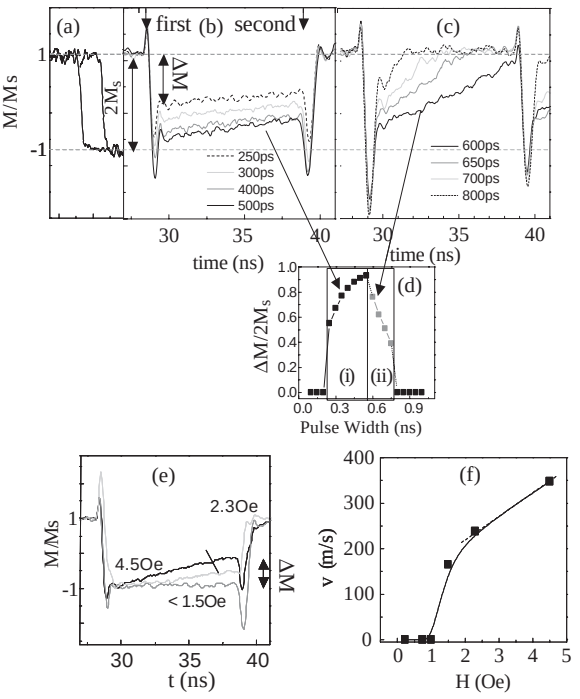

Fig. 3. (a) The static M–H loop for the Py film defining the saturation levels. (b, c) Time traces at $h_p = 42$ Oe and $H_b = 1.6$ Oe with pulse widths corresponding to (a) the 1st reversal regime and (b) the transition to the 2nd non-reversal regime, as indicated in (d) by the relative signal level change $\Delta M/2M_s$ vs. pulse width. (e) Time traces for different H_b. (f) Wall velocity vs. H_b (the line is a guide to the eye). The over- and undershoots seen in (a) and (b) beyond the static magnetisation levels are attributed to an optical effect.

the two field pulses is not constant but increases towards the upper magnetisation level. Depending on the pulse duration, this increase is either (i) linear and 'slow' as in Fig. 3a (partial back reversal in 10 ns) or (ii) stronger than linear and 'fast' as in Fig. 3b (complete back reversal in 10 ns). The pulse width durations of these two types of 'relaxation' processes coincide with the 1st reversal regime, see Fig. 3d, and respectively with the transition from the 1st reversal to the 2nd non-reversal regime.

The relaxation in case (i) can be explained by domain wall motion at constant velocity. Since the magnetisation reversal occurs only in a stripe of about 18 μm, a domain of this width is created, separated by two domain walls from the non-excited region, see Fig. 1. The bias field then applies a pressure onto the domain walls and

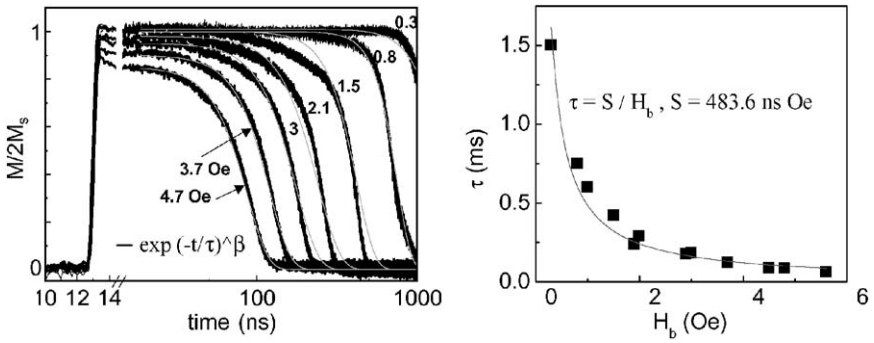

Fig. 4. (a) Time traces of the Finemet film for different H_b and (b) switching time τ vs. H_b , from which the switching parameter S is deduced.

pushes the domain walls towards the centre of the stripe, which is probed by the laser spot. This behaviour is substantiated, by the linear decrease of the magnetisation level as a function of the bias field H_b. In Fig. 3e different time traces are shown for different H_b. For $H_b < H_c$, there is no relaxation and the magnetisation level remains constant, while for $H_b > H_c$ the slope of the magnetisation increases with H_b. From this variation, the domain wall velocity can be estimated, if one assumes for a first approximation that the two domain walls are straight over the 15 μm laser spot and move symmetrically under the laser spot. The total signal change after 10 ns for the displacement of two walls is $\Delta M/2M_s$. This is equal to the relative change in area $\Delta A/A$ of the reversed domain inside the circular laser spot, assuming a symmetric and linear displacement Δx of both domain walls. With $\Delta A/A = 2\Delta x/D$, and D the spot diameter we obtain $\Delta M/2M_s = 2\Delta x/D$. From this the wall velocity $v = \Delta x/\Delta t$ is deduced. The results are shown in Fig. 3f. The curve reflects the conventional relation of $v = \mu^*(H_b - H_c)$, with H_c corresponding to the coercive field as measured from static M–H loops. From the high field slope the wall mobility μ is estimated $\mu = 44$–56 m/Oe s, which is in the range of values published in literature. For example the wall mobility given for FeNi micron sized wires is 2.6 (m/Oe s) [7] and for epitaxial Fe/Ag thin films 117 (m/Oe s) [8].

In contrast to the linear relaxation in the reversal regime (i), the stronger than linear behaviour in regime (ii), Fig. 3b, needs further investigation. In this regime the magnetisation rotates back towards the initial magnetisation direction. It appears that the magnetisation does first stabilise in an intermediate orientation before finally relaxing towards the initial direction. More studies are required in order to elucidate whether this corresponds to wall motion and/or a rotational relaxation.

Finally, it is noted that the relaxation in the Finemet sample showed a completely different behaviour. The observed magnetisation variation is more consistent with a thermally activated relaxation following a stretched exponential decay with decreasing relaxation time τ for increasing H_b. This is shown in Fig. 4a, where time traces are plotted for different applied bias field. From fits using a stretched exponential the relaxation time for each applied bias field H_b is determined as plotted in Fig. 4b. As can be seen τ is inversely proportional to H_b and follows the general behaviour of $\tau = S/H_b$. Here S is the switching coefficient which is estimated to 483.6 ns/Oe. The reason for this thermally activated behaviour needs further investigation, but is thought to be related to the crystalline structure of the precursor alloy, which most likely provides a high density of pinning sites.

Acknowledgements

This work was supported in part by the European programme HPRN-CT-2002-00289

DYNAMICS. The authors wish to acknowledge the support from NANOFAB2000/CNRS for the optical lithography of the CPW and B. Rodmacq and S. Auffret for the FeNi sample preparation.

References

[1] J. Miltat, G. Albuquerque, A. Thiaville, in: B. Hillebrands, K. Ounadjela (Eds.), Spin Dynamics in Confined Magnetic Structures, vol. I, Springer, Berlin, 2000.
[2] S. Kaka, S.E. Russek, Appl. Phys. Lett. 80 (2002) 2958.
[3] W.K. Hiebert, L. Lagae, J. Das, J. Bekaert, R. Wirix-Speetjens, J. De Boeck, J. Appl. Phys. 93 (2003) 6906.
[4] H.W. Schumacher, C. Chappert, P. Crozat, R.C. Sousa, P.P. Freitas, J. Miltat, J. Fassbender, B. Hillebrands, Phys. Rev. Lett. 90 (2003) 17201.
[5] T. Gerrits, et al., Nature 418 (2002) 509.
[6] T. Devolder, C. Chappert, Eur. Phys. J. B 36 (2003) 57.
[7] T. Ono, H. Miyajima, K. Mibu, et al., Science 284 (1999) 486.
[8] R.P. Crowburn, J. Ferré, Appl. Phys. Lett. 74 (1999) 1018.